ACS APPLIED MATERIALS & INTERFACES

www.acsami.org

Research Article

On-Demand Maneuver of Millirobots with Reprogrammable Motility by a Hard-Magnetic Coating

Longfu Li, Chen Xin, Yanlei Hu,* Rui Li, Chuanzong Li, Yachao Zhang, Nianwei Dai, Liqun Xu, Leran Zhang, Dawei Wang, Dong Wu, Changrui Liao,* and Yiping Wang

Cite This: *ACS Appl. Mater. Interfaces* 2022, 14, 52370−52378

Read Online

ACCESS | Metrics & More | Article Recommendations | Supporting Information

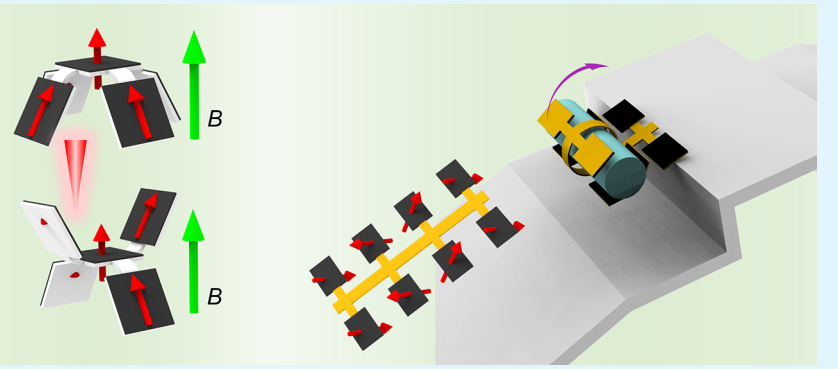

ABSTRACT: Millirobots that can be actuated and accurately steered by external magnetic fields, are highly desirable for bioengineering and wearable devices. However, existing designs of millirobots are limited by their specific material composition, hindering their wider application due to a lack of scalability. Here, we present a method for the generation of heterogeneous magnetic millirobots based on magnetic coatings. The coatings, composed of hard-magnetic CrO_2 particles dispersed in an adhesive solution, impart magnetic actuation to diverse substrates with planar sheets or 3D structures. Millirobots constructed from the coatings can be readily reprogrammed with intricate magnetization profiles using laser localized heating, enabling reconfigurable shape changes under magnetic actuation. Using this approach, we demonstrate on-demand maneuvering capability of reconfiguring locomotion involving crawling, overturning and rolling with a single millirobot. Various functions, including the ability to catch a fast-moving ball, object transportation, and targeted assembly, have been achieved. This adhesive strategy facilitates the design of millirobots and may open avenues to the creation of complex millirobots for broad applications.

KEYWORDS: *magnetic actuation, magnetic domains, reprogrammable magnetization, locomotion, millirobots*

INTRODUCTION

Millimeter-scale robots hold great potential in the fields of bioengineering, healthcare, and environmental monitoring.[1−3] The development of responsive materials enables millirobots to convert external stimulus such as light,[4−6] heat,[7] pH,[8] humidity,[9] and electrical[10] and magnetic fields[11−14] into mechanical movements. Among these stimuli, magnetic fields, with distinct advantages of being fast, precise and safe, offer an untethered way to dexterously manipulate the responsive machines.[15] The mechanism to activate and manipulate the magnetic robots relies on the magnetic force and torque exerted on magnetic components. To be more specific, their motion capability and functionality are dependent on the localized distribution of magnetic moments in the robots. Therefore, precise realization of programmable and reconfigurable magnetic moments in arbitrary sites are highly desirable for effective control and enriched functionality of magnetic millirobots.

Discrete magnetic millirobots provide a straightforward way toward magnetically drivable operation, in which discrete tiny magnets or patches of magnetic composite are affixed to deformable body as guiding components for programmed magnetic assembly and actuation.[16−20] Nevertheless, the non-negligible footprint increases as a result of numerous discrete magnets and the limited flexibility in magnetic programming hinders further miniaturization and implementation of such millirobots.

On the contrary, continuous magnetic millirobots incorporating micro/nanomagnetic particles in a soft polymeric matrix

Received: August 8, 2022
Accepted: October 31, 2022
Published: November 9, 2022

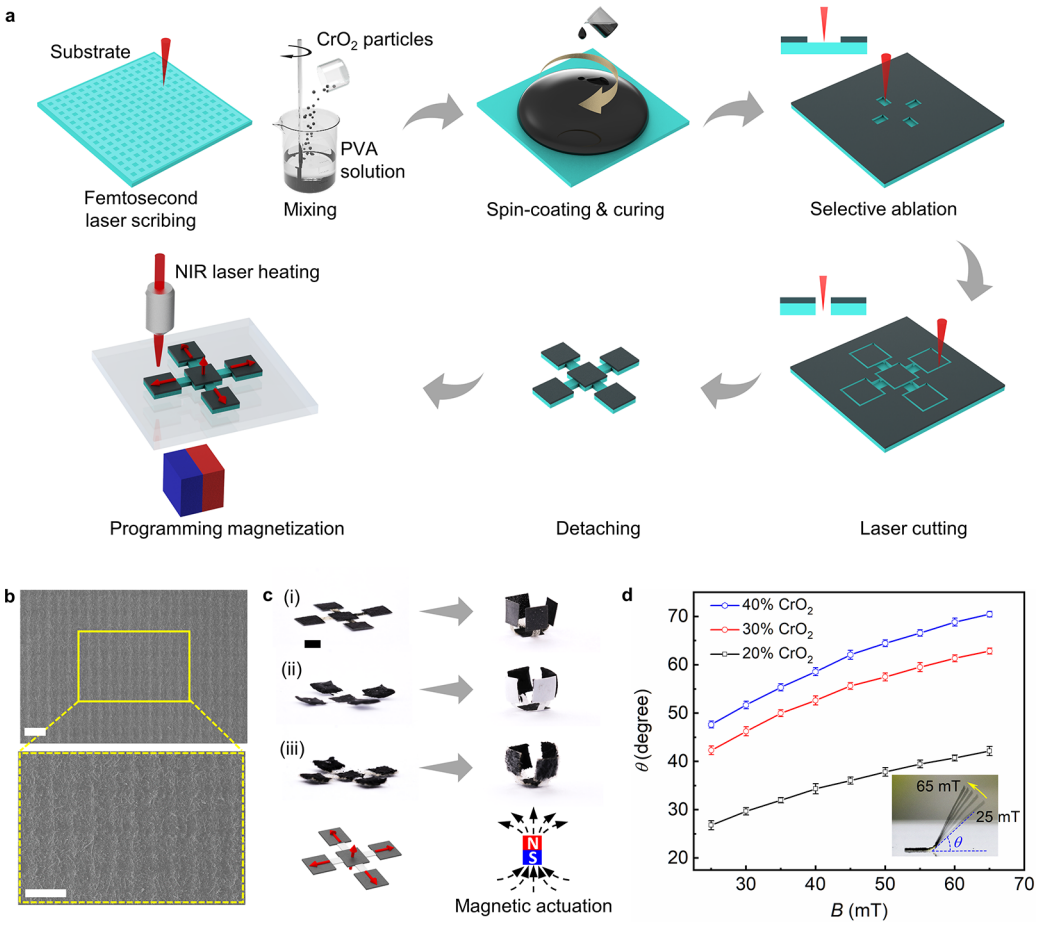

Figure 1. Magnetic coating turning nonmagnetic objects into millirobots. (a) Schematics showing the preparation of millirobots involving microgrooves induced by femtosecond laser ablation, dissolution of CrO_2 particles into PVA solution, spin-coating, removal of partial area of coatings and geometry cutting by femtosecond laser, and magnetic programming assisted by laser heating. (b) Microscopic images displaying the morphology of microgrooves generated by femtosecond laser ablation. Scale bars, 100 μm. (c) Realization of shape change of a sheet of (i) TPU, (ii) paper, and (iii) nonwoven fabric substrate under an upward magnetic field when coated with a magnetic film onto its surface. The image in the lower left is a schematic of the magnetization profile, where the magnetization directions are marked with red arrows. Scale bar, 2 mm. (d) Dependence of the folding angles of strips on both the magnetic flux density strength and the loading percentage of CrO_2 particles in the magnetic coatings, which are performed by using strips of identical structures, whose geometry sizes are 9 mm long and 2 mm wide. The inset photograph shows the actuation performance of a strip (with coatings of 30% CrO_2) under varied magnetic fields from 25 to 65 mT (ΔB = 10 mT).

offer extra opportunities in flexibility and versatility. By introducing magnetic anisotropy in the magnetic composites, morphological transformations of millirobots can be accomplished. Programming magnetic anisotropy has been achieved by physical alignment of soft-magnetic particles to form a chainlike microstructure,[21−23] or by orientation of premagnetized hard-magnetic particles toward the designated direction,[24−28] both of which resulted from a magnetic field being applied to immobilize magnetic fillers in polymeric matrices during the fabrication process such as template-assisted curing, 3D printing or UV lithography. Furthermore, reprogrammable magnetic anisotropy endows a magnetic actuator with the capability of multiple shape changes upon an identical magnetic field. To date, three different kinds of reprogramming strategies have been introduced based on reorientating the magnetic particles embedded in fusible polymeric matrices,[29,30] applying a magnetic field greater than coercivity,[31−33] and heating the ferromagnet above its Curie temperature followed by a magnetization process during cooling.[34] However, the existing reprogrammable magnetic millirobots mostly feature homogeneous materials in a planar form, which imposes great constrains on materials universality, design freedom, and functionality. Although assembly approaches based on thermal welding or bonding agents can tackle these issues to a certain extent, the applicability of substrate materials is still limited to a few elastomers.[35,36]

Recently, adhesive strategies emerge as a promising route to construct heterogeneous magnetic millirobots by expediently integrating responsive adhesive layers with diverse substrates.[37,38] It holds the outstanding merits of adapting to arbitrary structures regardless of material, shape and scale. In particular, an agglutinated spray of magnetic composite is invented to functionalize inanimate surfaces.[37] Although the use of soft-magnetic iron microparticles results in inevitable limitations in magnetic moment design (no magnetic repulsion can be generated) and difficulty in effective reprogramming in an atmospheric environment, it provides researchers with vast inspiration for developing designable functional magnetic millirobots based on the adhesive strategy.

Here, we report a coating-based approach to preparing heterogeneous magnetic millirobots from diverse nonmagnetic substrates. This approach is enabled by stable adhesiveness of

https://doi.org/10.1021/acsami.2c14180
ACS Appl. Mater. Interfaces 2022, 14, 52370−52378

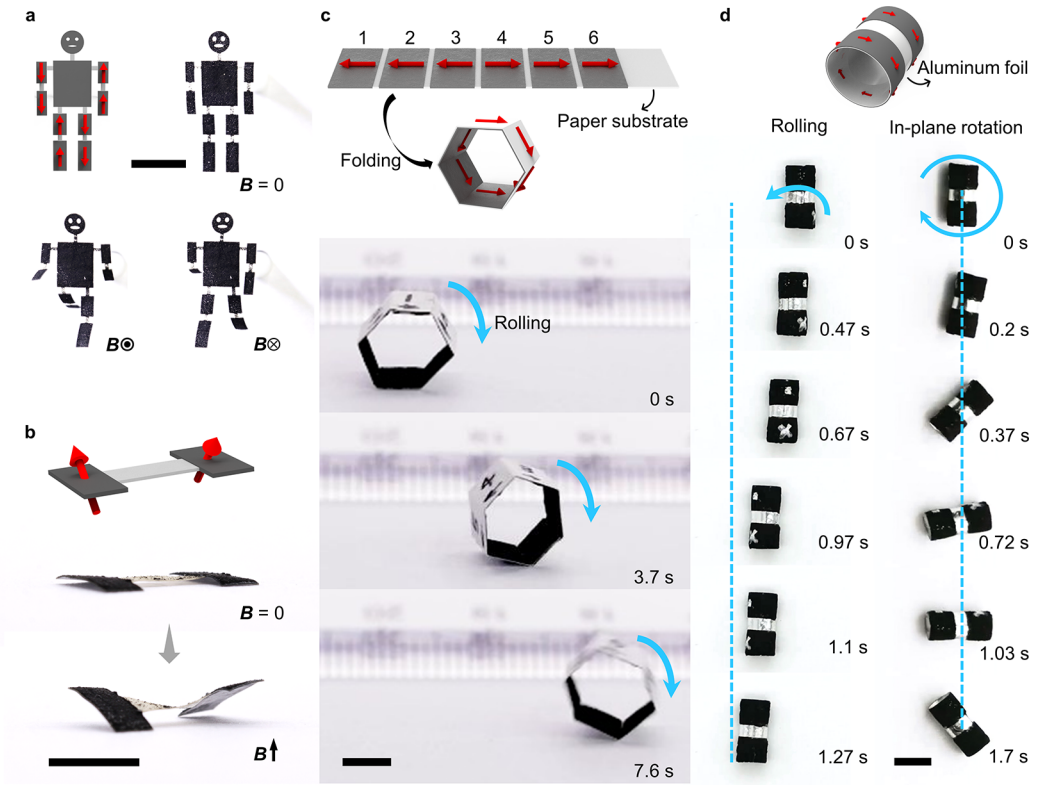

Figure 2. Programmable 3D magnetization directions, shape deformation, and controlled locomotion of diverse substrates. (a, b) Examples of the magnetic patterns and the corresponding (a) pedestrian-like structure and (b) twisting structure upon a magnetic field of 60 mT, both of which are composed of a sheet of TPU and the magnetic coatings on their surfaces. (c) Hexagonal tube made of paper and the magnetic coatings on its inner surface via an origami technique, whose magnetization profile is encoded at the deployed state, generates a forward rolling motion with rotational magnetic actuation. (d) Circular tube structure consisting of aluminum foil and the magnetic coatings on the outer surface is programmed with magnetization directions along the tangential direction of the circumference. Scale bars, 5 mm.

magnetic coatings to the surface of objects from planar sheets to 3D structures. By virtue of the hard-magnetic coatings, programmable and reconfigurable magnetization profiles with arbitrary discrete magnetic moments can be readily patterned by means of laser localized heating, giving rise to the accurate steerability and locomotion diversity of millirobots. Taking advantage of this method, reconfigurable shape transformation and tunable locomotion modes of one structure with on-demand manipulation capabilities are demonstrated. Furthermore, diverse manipulation functions, including the capture of moving objects, transportation, and assembly have been achieved. Our fabrication scheme provides a rapid and facile tool to turn multiple inanimate materials into millirobots, thereby establishing a new route to design millirobots.

RESULTS AND DISCUSSION

Characterization of Magnetic Coating. Our magnetic composite is prepared by suspending CrO_2 particles in PVA solution, and then the magnetic slurry of CrO_2@PVA composite is coated on the surface of a targeted object followed by a solidifying process. CrO_2 particles stably exists on the surface of an object without any chemical changes after being subjected to the solidifying process (Figure S1). During the solidifying process, the magnetic coating gradually solidifies to a form of magnetic film as a result of the evaporation of water in PVA solution (Figure S2). The resultant thickness of the magnetic film is relevant to CrO_2 content, which varies from 50 to 105 μm when the CrO_2 content increases from 20 to 40% (Figure S2), suggesting a facile way to control the thickness of the film. The magnetic particles are evenly distributed without apparent aggregation on the surface of a substrate after solidification, as indicated by the scanning electron microscopy (SEM) images (Figure S2).

Microgrooves are generated on the smooth surfaces of hydrophobic materials such as polyurethane (TPU) and polydimethylsiloxane (PDMS) by femtosecond laser ablation (Figure 1b) in order to enhance the adhesion of the magnetic coating to their surfaces, as a rough surface possesses stronger adhesion strength than a smooth one.[37] To demonstrate the adhesive ability of the magnetic coating to diverse materials, we coated the magnetic slurry onto different substrates with an identical structure. Experimental results show that the magnetic coating exhibits stable and firm adhesion to the surface of a wide range of substrates like TPU, paper, cloth, and metal (Figure 1c). The strong hydrogen bonds between PVA chains and water imparts the magnetic coating with high wetting and strong adhesive abilities.[37,39] Moreover, it undergoes a paste−solid transition after solidification and thus become nonviscous to other surfaces. Therefore, the effective adhesion ability before solidification, together with the magnetic actuation performance after solidification, make the magnetic film an efficient tool to construct millirobots from nonmagnetic objects.

Strategy to Construct Millirobots from Nonmagnetic Objects. In our strategy, it takes two steps to construct a magnetically drivable robot: coating the object with a magnetic film and then programming magnetic anisotropy on the film. A flexible substrate coated with the magnetic film is cut into a designed geometry, where a femtosecond laser is used to remove

https://doi.org/10.1021/acsami.2c14180
ACS Appl. Mater. Interfaces 2022, 14, 52370−52378

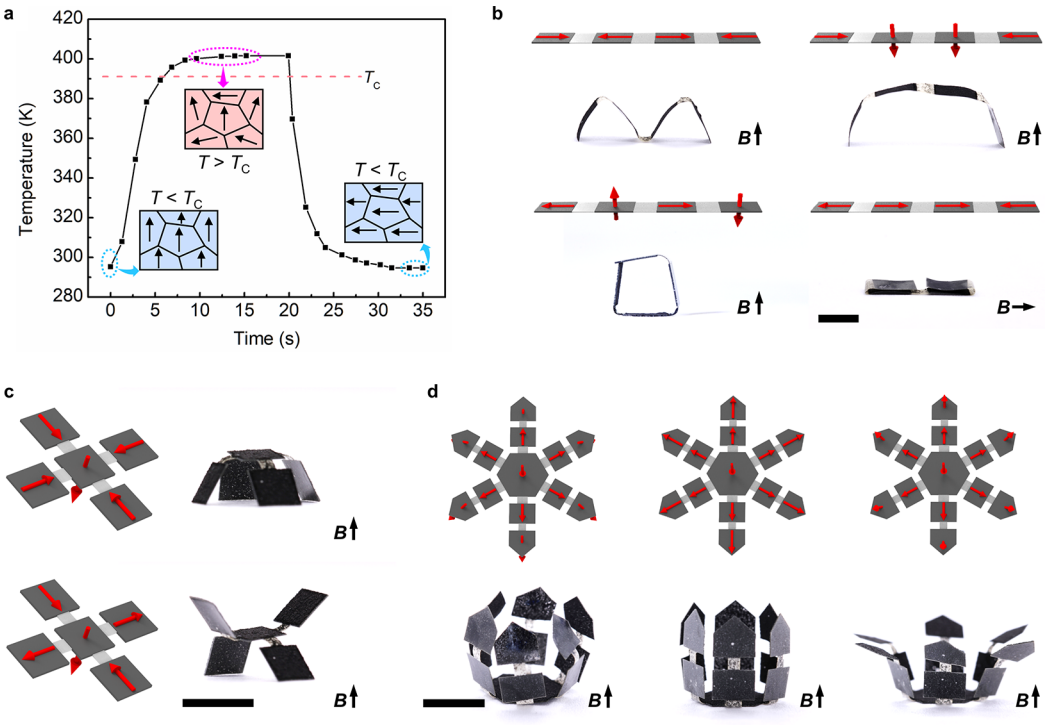

Figure 3. Reprogrammable magnetization profiles and shape changes. (a) Schematic illustration of magnetic reprogramming showing reorientation of magnetic domains during the process of NIR-assisted magnetization, where the laser power is set at 175 W. (b–d) Schematic description of the magnetic patterns and the corresponding shape changes upon application of magnetic fields. The upward magnetic fields are generated by a permanent magnet located (c) below and (d) above the robots. Scale bars for all images: 5 mm.

the upper magnetic film to form joints between adjacent segments. Such structural designs are adopted mainly for two reasons. First, it is constrained by the magnetic film which becomes nondeformable after paste–solid transition. Second, folding around the joints is more energetically efficient than homogeneous bending of the whole structure, as revealed by a recent study.[40] Figure 1c presents diverse substrates such as TPU, paper, and nonwoven fabrics in response to external magnetic fields, where all the substrates are designed with planar segments connected via flexible joints. The designated magnetization profiles are programmed via a heat-assisted magnetization strategy by means of near-infrared (NIR) laser localized heating (described in Text S1), enabling arbitrary discrete magnetic moments. Consequently, by virtue of the deformable substrates as joints, each planar segment folds under magnetic actuation.

To quantitatively assess the performance of magnetic actuation, we encoded a strip of TPU substrate with a joint on the left side with in-plane magnetization directions along its length and subjected to a magnetic field applied perpendicular to the plane (Figure 1d). A folding angle, θ, which characterizes the performance of the strip in response to magnetic fields, increases linearly from 42.3 to 62.9° as the magnetic field varies from 25 to 65 mT (Figure 1d), indicating a good performance of the magnetic film intended for accurate actuation of objects. A magnetically patterned segment experiences a magnetic torque in the presence of an external magnetic field, in which the segment tries to align its magnetization direction with the field direction, leading to folding (or rotating) around a joint. As shown in Figure 2a, a cartoon figure patterned with in-plane magnetization directions for its extremities mimics a pedestrian when exposed to an alternating magnetic field normal to the plane. When the shape of a dumbbell-like plane structure is encoded with discretely out-of-plane magnetization profiles, it deforms into 3D structure, giving rise to a twist of the flexible substrate in the middle under a magnetic field of 60 mT perpendicular to the plane (Figure 2b). It is worth noting that the deformations of the structures can result from both attractive and repulsive forces exerted on the magnetic film, which is attributed to the existence of remanent magnetization of CrO_2 particles and hence is distinctly different from the deformation modes based solely on attractive forces acting on the soft-magnetic particles like Fe and Fe_3O_4.[21,22,37] Therefore, compared with robots covered with soft-magnetic films, a robot covered with hard-magnetic coating exhibits higher degrees of freedom and superior design flexibility, making more complex deformation modes possible.

In the case of rigid substrates, an object is always divided into several regions and discretely patterned via a heat-assisted magnetization approach or through keeping small-sized magnets in close proximity, enabling locomotion modes like rolling, rotating, and tumbling. The force for rolling and rotating motion arises from the magnetic torque, whereas the magnetic force is responsible for steering the rolling direction. Figure 2c depicts a hollow hexagonal tube created based on origami techniques. Its in-plane magnetization directions are patterned at the deployed state, giving rise to the formation of desired magnetizations in varying 3D directions once folded. When a cubic permanent magnet underneath the hexagonal tube rotates counterclockwise around the axis of the hexagonal tube, the hexagonal tube rolls forward clockwise at a pace of 60 deg/step (Video S1). It is worth noting that this approach for programming spatially distributed magnetization directions is applicable for any substrates such as paper sheet as well as metallic foil, as long

https://doi.org/10.1021/acsami.2c14180
ACS Appl. Mater. Interfaces 2022, 14, 52370–52378

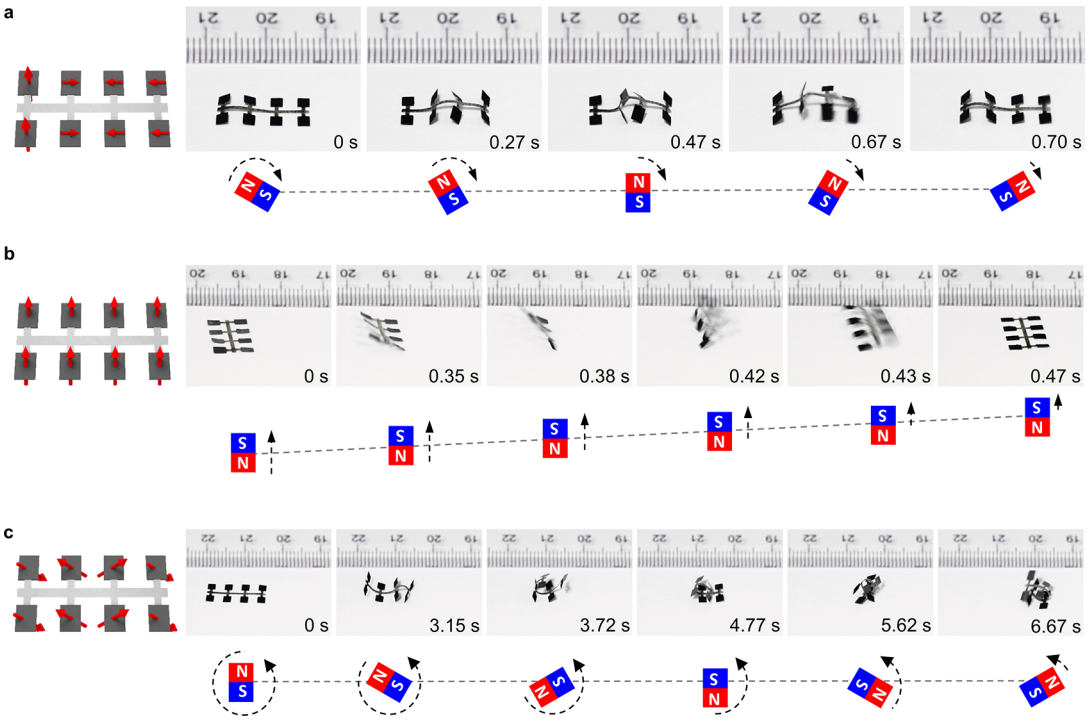

Figure 4. Locomotion modes of an eight-legged millirobot with distinct magnetic patterns enabled by reprogramming: (a) crawling motion, (b) overturning motion, and (c) rolling motion.

as they can be folded along their creases to form a 3D structure. Similarly, a circular tube made of aluminum foil is fabricated and is driven to roll forward/backward around its own axis under an out-of-plane counterclockwise/clockwise rotating magnetic field, whereas it rotates simultaneously as a permanent magnet rotates about the normal direction of the plane (Figure 2d and Video S2).

Reprogrammable Magnetization. Reprogrammable magnetization is beneficial to millirobots by maximizing their shape deformation and locomotion modes, endowing them with higher programming freedom and better environmental adaptability. Reprogrammable magnetization of the robots is enabled by the CrO_2 magnetic film through reorientation of the magnetic domains. As shown in Figure 3a, the magnetic domains orientate orderly in the ferromagnetic state below the Curie temperature (T_C), whereas they orientate randomly at higher temperatures above T_C. In addition, the ordered magnetic domains can be reorientated upon application of a magnetic field when they undergo a transition from the paramagnetic state ($T > T_C$) to the ferromagnetic state ($T < T_C$). As a result, magnetic reprogramming is attainable based on this heat-assisted magnetization strategy. Since the Curie temperature of CrO_2 (T_C = 391 K) is well within the operating temperature range of most materials,[11] minimal impact would be imposed on the properties of substrates. More importantly, the heat-assisted magnetization approach allows a facile and efficient way of magnetic reprogramming that does not require any extra treatments of the magnetic film and substrates, completely different from previous robots constructed with iron-skin magnetic film which depend on physical realignment of the embedded magnetic particles at wet or liquid environment.[37] Thus, more complex morphologies and shape transformations are easily attainable. Figure 3b presents a 1D strip of TPU substrate fabricated with the magnetic films coated onto four divided sections. For the strip encoded with in-plane alternating magnetization directions, an 'm'-like shape is obtained upon an upward magnetic field. When two middle sections of the strip are reprogrammed with magnetization directions opposite to the magnetic field, the strip undergoes a gate-like shape transformation under magnetic actuation. Similarly, more shape-morphing configurations can also be realized by reprogramming its magnetization profiles, as shown in Figure 3b. Additionally, a planar structure can transform into various 3D structures using this heat-assisted magnetization approach. Figure 3c shows two distinct conformations tailored by reprogramming different magnetic configurations in the five panels. Moreover, multiple conformations can also be obtained by subtly reprogramming the magnetization directions. As a demonstration, a six-armed millirobot is designed (Figure 3d). The different magnetization directions of the outer six panels enabled by magnetic reprogramming make it exhibit three different morphological structures.

Reprogrammable magnetization can be further explored to optimize the motion behaviors of robots by creating different magnetization profiles. Figure 4 shows an eight-legged millirobot made of a TPU substrate with the magnetic films coated solely onto eight legs. The magnetic films provide magnetic torque and propulsive forces to drive shape morphing of the flexible body and locomotion of the whole structure. On the basis of the facile magnetic reprogramming of the films, the millirobot is subsequently encoded with three distinct magnetic patterns. Therefore, the millirobot exhibits reconfigurable locomotion modes, i.e., crawling, overturning, and rolling. A cubic magnet is placed underneath the millirobot, which provides magnetic torque and force to drive the robot to locomote on the plane. A crawling motion mimicking an inchworm based on out-of-plane bending is realized once the millirobot is exposed to a magnetic field swinging back and forth (Figure 4a). When the magnet swings back and forth within a certain angle range, a spatiotemporally varied magnetic field is

https://doi.org/10.1021/acsami.2c14180
ACS Appl. Mater. Interfaces 2022, 14, 52370−52378

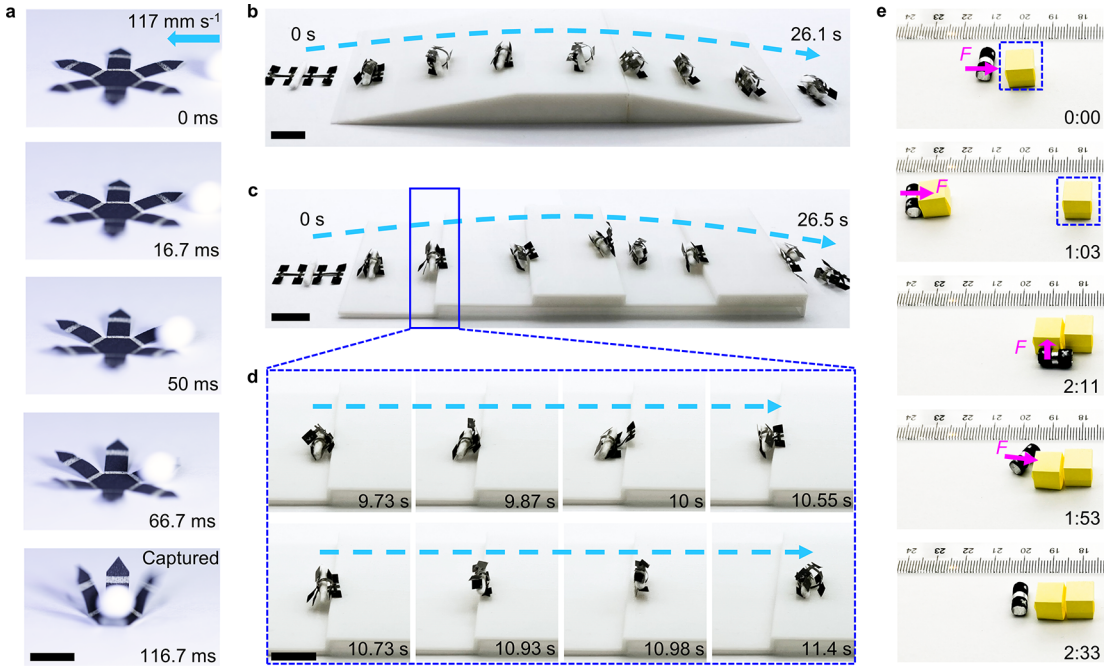

Figure 5. Functional demonstrations of flexible and rigid robots with programmed magnetization profiles. (a) Snapshots showing that a gripper structure made from flexible TPU substrate catches a fast-moving ball upon application of an upward magnetic field. The base of the gripper structure is fixed to the platform to guarantee a stable shape transformation. (b,c) Frames from recorded videos illustrating that an eight-legged millirobot holds a rod-like object for transportation based on rolling locomotion through different terrains, including (b) slopes and (c) various steps. (d) Details extracted from the same video as shown in panel c represent the way an eight-legged millirobot climbs over an obstacle with a height of 4 mm while keeping the object being tightly wrapped. (e) Magnetically controlled manipulation and assembly by using a tube fabricated with rigid aluminum foil and magnetic coatings on its surface. The time stamp format is minutes:seconds. Scale bars: (a) 5 mm, (b) 10 mm, (c) 10 mm, and (d) 10 mm.

produced. Consequently, as the magnetic field sweeps from right to left, the magnetic torque exerted on six legs on the right drives them to bend and deform the body. In the meanwhile, the time-varying magnetic field causes the body to constantly bend toward the middle of the robot, whereas two outer legs on the far left basically remain stationary, forming an overall arched structure. In contrast, when the magnetic field turns from left to right, the robot is unfolded from left to right by the action of the magnetic torque, thereby driving the entire robot to move forward (i.e., to the right side) for a certain distance. Therefore, this bending-unfolding process generates a net displacement that drives the entire robot forward. By repeating the magnetic actuation process successively, the robot moves forward in a crawling motion, resulting in a distance of 8.5 mm in five cycles (Video S3). When all legs are reprogrammed with an identical magnetization direction at an angle of 45° to the normal vector of the plane (Figure 4b), the movement efficiency of the robot can be markedly enhanced. The robot overturns upon a magnetic field perpendicular to the plane, making it move forward by a distance of 9 mm in each cycle (1 BW/cycle, BW: body width). Consequently, the robot keeps advancing continuously in an overturning motion by alternately applying magnetic fields in the upward and downward directions (Video S3). Furthermore, the legs can also be reprogrammed with discretely 3D magnetization directions in the normal plane along the length of the robot (Figure 4c). Correspondingly, the robot gradually curls into a tubular shape under the action of a counterclockwise rotating magnetic field generated by a rotary magnet underneath. Further, moving the magnet forward as it rotates allows the robot to continuously roll forward (Video S3). Compared with the first two locomotion modes, the rolling motion enables the robot to transform between planar and 3D structures, allowing for better adaptability to different terrains and unstructured environments. Moreover, the curled tubular structure facilitates carrying and transporting objects in the movement, as discussed in the following section.

On-Demand Maneuvering and Functionality. The ability of the magnetic coatings to actuate diverse substrates enables us to achieve various functions based on the deformation and motion from the structures. As shown in Figure 5a, an articulated gripper that has a base, six arms, and six fingers with a centrosymmetric structure forms a semiclosed structure in response to an upward magnetic field. It is worth noting that although the first two magnetization profiles as shown in Figure 3d both form semiclosed structures in an upward magnetic field, the latter involving the same magnetization directions in its adjacent arms and fingers somewhat exhibits faster and more stable magnetic actuation. Therefore, both the arms and fingers of the gripper are programmed with in-plane magnetization directions (Figure S6). By virtue of its rapid response to an external magnetic field, a fast-moving Telfon ball at a speed of 117 mm/s is captured (Video S4).

The multilegged robot can be further explored for object transportation based on the rolling locomotion displayed in Figure 4c. Harnessing the shape deformation and motion of the robot, rod-shaped objects can be held tightly in the tubular structure while the robot is rolling forward, whereas the release of an object can be readily attained by stretching the robot when the magnetic field is removed. Controlled rolling locomotion of the robot carrying an object for climbing up and down ramps of 11° is realized (Figure 5b; Video S5). We further design a series of steps, a 3 mm deep trench, and a steep drop of 7 mm to the countertop at the end of them. The results in Figure 5c demonstrate that the robot is able to carry objects through these

https://doi.org/10.1021/acsami.2c14180
ACS Appl. Mater. Interfaces 2022, 14, 52370−52378

obstacles. More impressively, the object is tightly wrapped in the robot's tube structure even when the robot rolls down from the high drop (Video S5). As shown in Figure 5c and d, when the robot approaches an obstacle like a step or a trench, it places a pair of legs at the front of its body on the upper end of the obstacle. Then, taking advantage of the support provided by the front legs for the whole body, the robot continues to roll up its body under the rotating magnetic field to overcome these obstacles. Since only six legs on the left of the robot are required to wrap the object, an object will not fall off the robot during the transportation process and over obstacles.

We further demonstrate the capability of orientation control of an untethered rigid tubular robot for intentional manipulation and assembly of objects (Figure 5e; Video S6). A robot composed of a rigid base can be operated to manipulate objects larger than itself with the help of the forward propulsion of its rigid body. This strategy allows the tubular robot to simply push objects to desired locations. In Figure 5e, two cubes are pushed to a prescribed position for assembly in a straight line. In fact, this approach of robotic manipulation can be extended to handle object units of different shapes into various final geometrical patterns such as triangle and rod patterns, as well as into composites forms with heterogeneous structures.[41] These results suggest the potential application of untethered robotic assembly for coding and repair of millimeter-scale components constrained by energy supply.

CONCLUSIONS

In summary, this work introduces an approach to creating magnetically drivable millirobots from various nonmagnetic objects by covering them with hard-magnetic coatings. This method enables different substrates ranging from planar sheets to 3D structures to be effectively actuated under magnetic fields. When combined with NIR laser heating, the millirobots can be reprogrammed with arbitrary magnetization patterns in a rapid and facile fashion. By leveraging this method, multiple locomotion modes like crawling, overturning, and rolling, as well as good magnetic steerability and manipulation capabilities, are demonstrated. Various functions of these millirobots have been achieved, including catching a fast-moving object, object transport and assembly. Although functional applications in aqueous environment is limited by the stability of the magnetic coating in the current state, adding gluten as the component and an additional PVA layer can help build robust magnetic coatings, laying the foundation for possible application in such circumstances. The method described here is expected to provide alternative solutions to the design of millirobots.

MATERIALS AND METHODS

Sample Fabrication. The PVA with an 87.0 to 89.0% degree of alcoholysis and an average molecular weight of 85 000−124 000 was bought from Aladdin Chemistry Co. Ltd. Poly(vinyl alcohol) (PVA) aqueous solution (10 wt %) was obtained by stirring the mixture of PVA powders and deionized water at a mass ration of 1:9 under 98 °C for 3 h to ensure a complete dissolution. Then, the slurry of our magnetic composite was prepared by suspending CrO_2 particles (Aladdin Inc., China) in PVA solution with a predetermined mass ratio at room temperature. Then, the CrO_2@PVA slurry was coated on the surface of a targeted object (TPU, PDMS, paper, and nonwoven fabric) at 500 rpm for 30 s, followed by a solidifying process for 30 min at 40 °C. Besides, for some objects of 3D structures like the circular tube made of aluminum foil, the magnetic coating was formed by simply spreading the magnetic slurry on its outer surface.

A femtosecond laser system (Legend Elite-1K-HE, Coherent) was employed for ablation and cutting. Femtosecond laser ablation was applied to constructing microgrooves to strengthen the adhesion of magnetic coatings to hydrophobic materials like TPU and PDMS with smooth surfaces, where the laser power, scanning speed, and spacing was set at 300 mW, 20 mm/s, and 30 μm, respectively. In addition, femtosecond laser ablation was used to obtain joints from flexible substrates by removal of the upper magnetic film. Then, the desired geometries were cut out of the substrates.

To create the desired magnetization profiles, heat-assisted magnetic (re)programming strategy was employed. A sample was placed on an acrylic plate and covered by a glass slide to fix its position. A NIR laser was used to selectively heat the magnetic coating above the Curie temperature of the embedded magnetic particles. The power of the NIR laser was set at 175 mW, and the temperature of the magnetic coating can be heated up to 391 K in 6 s. Subsequently, the NIR laser was turned off to cool the magnetic coating. In concert with the cooling process was a magnetic field of 40 mT in a desired direction generated by a permanent NdFeB magnet underneath to (re)orientate the magnetic domains of the magnetic particles in the coatings. The orientation of the magnetic field was controlled by the rotation of the permanent magnet. Afterward, the sample was moved to a new laser-exposed region. By repeating this process, desired arbitrary magnetization directions were patterned on the magnetic coatings.

Sample Characterization. Room-temperature X-ray diffraction (XRD) measurements were performed on a Philips X'pert PRO X-ray diffractometer. The microstructure and morphology were characterized by a secondary electron SEM (ZEISS EVO18). The thickness of the magnetic coatings was measured using a step profiler (XP-1, Ambios Technology, Inc.). The magnetization was carried out on a Quantum Design vibrating sample magnetometer. The magnetic flux density was measured by a digital Gauss meter (HM-100, Huaming instrument Co., Ltd., China). A NIR laser (808 nm, 0−237 mW) was used for selectively local heating of magnetic coatings. The temperatures of the magnetic coatings were recorded by a thermal infrared camera (VarioCAMhr head 680, InfraTec).

Magnetic Actuation. A cube permanent magnet (25 mm wide) with a maximum magnetic flux density of 300 mT at its surface was utilized to form spatially distributed magnetic fields. Dynamic magnetic actuation was attained by moving the magnet in horizontal and vertical directions and/or by simultaneously involving a back-and-forth swinging or rotating motion of the magnet.

ASSOCIATED CONTENT

Supporting Information

The Supporting Information is available free of charge at https://pubs.acs.org/doi/10.1021/acsami.2c14180.

Mechanism of heat-assisted magnetization, strategy to construct millirobots from thick substrates, XRD patterns, size distribution of pristine CrO_2 particles, the solidifying process and thickness of magnetic coatings, microscopic morphologies of magnetic coatings, temperature dependent on laser power and time, magnetization hysteresis loops, schematic of magnetization profile (PDF)

Video S1: Controlled rolling motion of a hexagonal tube (MP4)

Video S2: Rolling and rotary motion of a circular tube (MP4)

Video S3: Reconfigurable motion of crawling, overturning, and rolling an eight-legged millirobot (MP4)

Video S4: Gripper structure catching a moving object (MP4)

Video S5: Object transportation over obstacles carried by a millirobot based on its rolling motion (MP4)

Video S6: Remote manipulation of a circular tube for magnetic assembly (MP4)

https://doi.org/10.1021/acsami.2c14180
ACS Appl. Mater. Interfaces 2022, 14, 52370−52378

AUTHOR INFORMATION

Corresponding Authors

Yanlei Hu − *CAS Key Laboratory of Mechanical Behavior and Design of Materials, Key Laboratory of Precision Scientific Instrumentation of Anhui Higher Education Institutes, Department of Precision Machinery and Precision Instrumentation, University of Science and Technology of China, Hefei 230027, China;* orcid.org/0000-0003-1964-0043; Email: huyl@ustc.edu.cn

Changrui Liao − *Key Laboratory of Optoelectronic Devices and Systems of Ministry of Education/GuangDong Province, College of Physics and Optoelectronic Engineering, Shenzhen University, Shenzhen 518060, China; Shenzhen Key Laboratory of Photonic Devices and Sensing Systems for Internet of Things, Guangdong and Hong Kong Joint Research Centre for Optical Fibre Sensors, Shenzhen University, Shenzhen 518060, China;* orcid.org/0000-0003-3669-5054; Email: cliao@szu.edu.cn

Authors

Longfu Li − *Key Laboratory of Optoelectronic Devices and Systems of Ministry of Education/GuangDong Province, College of Physics and Optoelectronic Engineering, Shenzhen University, Shenzhen 518060, China; Shenzhen Key Laboratory of Photonic Devices and Sensing Systems for Internet of Things, Guangdong and Hong Kong Joint Research Centre for Optical Fibre Sensors, Shenzhen University, Shenzhen 518060, China;* orcid.org/0000-0003-1685-7546

Chen Xin − *CAS Key Laboratory of Mechanical Behavior and Design of Materials, Key Laboratory of Precision Scientific Instrumentation of Anhui Higher Education Institutes, Department of Precision Machinery and Precision Instrumentation, University of Science and Technology of China, Hefei 230027, China*

Rui Li − *CAS Key Laboratory of Mechanical Behavior and Design of Materials, Key Laboratory of Precision Scientific Instrumentation of Anhui Higher Education Institutes, Department of Precision Machinery and Precision Instrumentation, University of Science and Technology of China, Hefei 230027, China*

Chuanzong Li − *School of Computer and Information Engineering, Fuyang Normal University, Fuyang 236037, China*

Yachao Zhang − *CAS Key Laboratory of Mechanical Behavior and Design of Materials, Key Laboratory of Precision Scientific Instrumentation of Anhui Higher Education Institutes, Department of Precision Machinery and Precision Instrumentation, University of Science and Technology of China, Hefei 230027, China*

Nianwei Dai − *CAS Key Laboratory of Mechanical Behavior and Design of Materials, Key Laboratory of Precision Scientific Instrumentation of Anhui Higher Education Institutes, Department of Precision Machinery and Precision Instrumentation, University of Science and Technology of China, Hefei 230027, China*

Liqun Xu − *CAS Key Laboratory of Mechanical Behavior and Design of Materials, Key Laboratory of Precision Scientific Instrumentation of Anhui Higher Education Institutes, Department of Precision Machinery and Precision Instrumentation, University of Science and Technology of China, Hefei 230027, China*

Leran Zhang − *CAS Key Laboratory of Mechanical Behavior and Design of Materials, Key Laboratory of Precision Scientific Instrumentation of Anhui Higher Education Institutes, Department of Precision Machinery and Precision Instrumentation, University of Science and Technology of China, Hefei 230027, China*

Dawei Wang − *CAS Key Laboratory of Mechanical Behavior and Design of Materials, Key Laboratory of Precision Scientific Instrumentation of Anhui Higher Education Institutes, Department of Precision Machinery and Precision Instrumentation, University of Science and Technology of China, Hefei 230027, China*

Dong Wu − *CAS Key Laboratory of Mechanical Behavior and Design of Materials, Key Laboratory of Precision Scientific Instrumentation of Anhui Higher Education Institutes, Department of Precision Machinery and Precision Instrumentation, University of Science and Technology of China, Hefei 230027, China;* orcid.org/0000-0003-0623-1515

Yiping Wang − *Key Laboratory of Optoelectronic Devices and Systems of Ministry of Education/GuangDong Province, College of Physics and Optoelectronic Engineering, Shenzhen University, Shenzhen 518060, China; Shenzhen Key Laboratory of Photonic Devices and Sensing Systems for Internet of Things, Guangdong and Hong Kong Joint Research Centre for Optical Fibre Sensors, Shenzhen University, Shenzhen 518060, China*

Complete contact information is available at: https://pubs.acs.org/10.1021/acsami.2c14180

Notes

The authors declare no competing financial interest.

ACKNOWLEDGMENTS

This work was supported by the National Natural Science Foundation of China (61927814, 52122511, 91963127, 51875544, 52105492, U20A20290), Major Scientific and Technological Projects in Anhui Province (201903a05020005, 202203a05020014), the University Synergy Innovation Program of Anhui Province (GXXT-2021-027), and the Fundamental Research Funds for the Central Universities (WK2090000024). We acknowledge the Experimental Center of Engineering and Material Sciences at USTC for the fabrication and measuring of samples. This work was partly carried out at the USTC Center for Micro and Nanoscale Research and Fabrication.

REFERENCES

(1) Sitti, M.; Ceylan, H.; Hu, W.; Giltinan, J.; Turan, M.; Yim, S.; Diller, E. Biomedical Applications of Untethered Mobile Milli/Microrobots. *Proc. IEEE* **2015**, *103* (2), 205−224.

(2) Ren, Z.; Zhang, R.; Soon, R. H.; Liu, Z.; Hu, W.; Onck, P. R.; Sitti, M. J. S. a. Soft-Bodied Adaptive Multimodal Locomotion Strategies in Fluid-Filled Confined Spaces. *Sci. Adv.* **2021**, *7* (27), No. eabh2022.

(3) Kim, Y.; Parada, G. A.; Liu, S.; Zhao, X. Ferromagnetic Soft Continuum Robots. *Sci. Robot.* **2019**, *4* (33), No. eaax7329.

(4) Liu, J. A.-C.; Gillen, J. H.; Mishra, S. R.; Evans, B. A.; Tracy, J. B. J. S. a. Photothermally and Magnetically Controlled Reconfiguration of Polymer Composites for Soft Robotics. *Sci. Adv.* **2019**, *5* (8), No. eaaw2897.

(5) Li, C.; Lau, G. C.; Yuan, H.; Aggarwal, A.; Dominguez, V. L.; Liu, S.; Sai, H.; Palmer, L. C.; Sather, N. A.; Pearson, T. J.; et al. Fast and Programmable Locomotion of Hydrogel-Metal Hybrids Under Light and Magnetic Fields. *Sci. Robot.* **2020**, *5* (49), No. eabb9822.

(6) Han, B.; Ma, Z. C.; Zhang, Y. L.; Zhu, L.; Fan, H.; Bai, B.; Chen, Q. D.; Yang, G. Z.; Sun, H. B. Reprogrammable Soft Robot Actuation by Synergistic Magnetic and Light Fields. *Adv. Funct. Mater.* **2022**, *32* (13), 2110997.
(7) Zhang, J.; Guo, Y.; Hu, W.; Sitti, M. Wirelessly Actuated Thermo- and Magneto-Responsive Soft Bimorph Materials with Programmable Shape-Morphing. *Adv. Mater.* **2021**, *33* (30), 2100336.
(8) Hu, Y. L.; Wang, Z. Y.; Jin, D. D.; Zhang, C. C.; Sun, R.; Li, Z. Q.; Hu, K.; Ni, J. C.; Cai, Z.; Pan, D.; Wang, X. W.; Zhu, W. L.; Li, J. W.; Wu, D.; Zhang, L.; Chu, J. R. Botanical-Inspired 4D Printing of Hydrogel at the Microscale. *Adv. Funct. Mater.* **2020**, *30* (4), 1907377.
(9) Gao, X.; Zhang, L.; Wang, S.; Yang, T.; Li, H. Soft Untethered Robots and Grippers Based on Humidity-Gated Magnetic-Responsive Film Actuators. *ACS Appl. Polym. Mater.* **2021**, *3* (9), 4726−4734.
(10) Wu, Y.; Yim, J. K.; Liang, J.; Shao, Z.; Qi, M.; Zhong, J.; Luo, Z.; Yan, X.; Zhang, M.; Wang, X.; et al. Insect-Scale Fast Moving and Ultrarobust Soft Robot. *Sci. Robot.* **2019**, *4* (32), No. eaax1594.
(11) Li, M.; Wang, Y.; Chen, A.; Naidu, A.; Napier, B. S.; Li, W.; Rodriguez, C. L.; Crooker, S. A.; Omenetto, F. G. Flexible Magnetic Composites for Light-Controlled Actuation and Interfaces. *Proc. Natl. Acad. Sci. U. S. A.* **2018**, *115* (32), 8119−8124.
(12) Wang, L.; Zheng, D.; Harker, P.; Patel, A. B.; Guo, C. F.; Zhao, X. Evolutionary Design of Magnetic Soft Continuum Robots. *Proc. Natl. Acad. Sci. U. S. A.* **2021**, *118* (21), No. e2021922118.
(13) Sun, M.; Tian, C.; Mao, L.; Meng, X.; Shen, X.; Hao, B.; Wang, X.; Xie, H.; Zhang, L. Reconfigurable Magnetic Slime Robot: Deformation, Adaptability, and Multifunction. *Adv. Funct. Mater.* **2022**, *32* (26), 2112508.
(14) Park, J. E.; Jeon, J.; Park, S. J.; Won, S.; Ku, Z.; Wie, J. J. Enhancement of Magneto-Mechanical Actuation of Micropillar Arrays by Anisotropic Stress Distribution. *Small* **2020**, *16* (38), 2003179.
(15) Ilami, M.; Bagheri, H.; Ahmed, R.; Skowronek, E. O.; Marvi, H. Materials, Actuators, and Sensors for Soft Bioinspired Robots. *Adv. Mater.* **2021**, *33* (19), 2003139.
(16) Kim, Y.; Zhao, X. Magnetic Soft Materials and Robots. *Chem. Rev.* **2022**, *122* (5), 5317−5364.
(17) Boncheva, M.; Andreev, S. A.; Mahadevan, L.; Winkleman, A.; Reichman, D. R.; Prentiss, M. G.; Whitesides, S.; Whitesides, G. M. Magnetic Self-Assembly of Three-Dimensional Surfaces from Planar Sheets. *Proc. Natl. Acad. Sci. U. S. A.* **2005**, *102* (11), 3924−3929.
(18) Gu, H.; Boehler, Q.; Ahmed, D.; Nelson, B. J. Magnetic Quadrupole Assemblies with Arbitrary Shapes and Magnetizations. *Sci. Robot.* **2019**, *4* (35), No. eaax8977.
(19) Miyashita, S.; Guitron, S.; Yoshida, K.; Li, S.; Damian, D. D.; Rus, D. Ingestible, Controllable, and Degradable Origami Robot for Patching Stomach Wounds. In *2016 IEEE International Conference on Robotics and Automation (ICRA)*; IEEE: Piscataway, NJ, 2016; pp 909−916.
(20) du Plessis d'Argentré, A.; Perry, S.; Iwata, Y.; Iwasaki, H.; Iwase, E.; Fabozzo, A.; Will, I.; Rus, D.; Damian, D. D.; Miyashita, S. Programmable Medicine: Autonomous, Ingestible, Deployable Hydrogel Patch and Plug for Stomach Ulcer Therapy. In *2018 IEEE International Conference on Robotics and Automation (ICRA)*; IEEE: Piscataway, NJ, 2018; pp 1511−1518.
(21) Kim, J.; Chung, S. E.; Choi, S. E.; Lee, H.; Kim, J.; Kwon, S. Programming Magnetic Anisotropy in Polymeric Microactuators. *Nat. Mater.* **2011**, *10* (10), 747−752.
(22) Huang, H. W.; Sakar, M. S.; Petruska, A. J.; Pane, S.; Nelson, B. J. Soft Micromachines with Programmable Motility and Morphology. *Nat. Commun.* **2016**, *7*, 12263.
(23) Jeon, J.; Park, J. E.; Park, S. J.; Won, S.; Zhao, H.; Kim, S.; Shim, B. S.; Urbas, A.; Hart, A. J.; Ku, Z.; Wie, J. J. Shape-Programmed Fabrication and Actuation of Magnetically Active Micropost Arrays. *ACS Appl. Mater. Interfaces* **2020**, *12* (14), 17113−17120.
(24) Lum, G. Z.; Ye, Z.; Dong, X.; Marvi, H.; Erin, O.; Hu, W.; Sitti, M. Shape-Programmable Magnetic Soft Matter. *Proc. Natl. Acad. Sci. U. S. A.* **2016**, *113* (41), No. E6007-E6015.
(25) Hu, W.; Lum, G. Z.; Mastrangeli, M.; Sitti, M. Small-Scale Soft-Bodied Robot with Multimodal Locomotion. *Nature* **2018**, *554* (7690), 81−85.
(26) Kim, Y.; Yuk, H.; Zhao, R.; Chester, S. A.; Zhao, X. Printing Ferromagnetic Domains for Untethered Fast-Transforming Soft Materials. *Nature* **2018**, *558* (7709), 274−279.
(27) Xu, T.; Zhang, J.; Salehizadeh, M.; Onaizah, O.; Diller, E. Millimeter-Scale Flexible Robots with Programmable Three-Dimensional Magnetization and Motions. *Sci. Robot.* **2019**, *4* (29), No. eaav4494.
(28) Zhang, Y.; Wang, Q.; Yi, S.; Lin, Z.; Wang, C.; Chen, Z.; Jiang, L. 4D Printing of Magnetoactive Soft Materials for On-Demand Magnetic Actuation Transformation. *ACS Appl. Mater. Interfaces* **2021**, *13* (3), 4174−4184.
(29) Deng, H.; Sattari, K.; Xie, Y.; Liao, P.; Yan, Z.; Lin, J. Laser Reprogramming Magnetic Anisotropy in Soft Composites for Reconfigurable 3D Shaping. *Nat. Commun.* **2020**, *11* (1), 6325.
(30) Song, H.; Lee, H.; Lee, J.; Choe, J. K.; Lee, S.; Yi, J. Y.; Park, S.; Yoo, J. W.; Kwon, M. S.; Kim, J. Reprogrammable Ferromagnetic Domains for Reconfigurable Soft Magnetic Actuators. *Nano Lett.* **2020**, *20* (7), 5185−5192.
(31) Cui, J.; Huang, T. Y.; Luo, Z.; Testa, P.; Gu, H.; Chen, X. Z.; Nelson, B. J.; Heyderman, L. J. Nanomagnetic Encoding of Shape-Morphing Micromachines. *Nature* **2019**, *575* (7781), 164−168.
(32) Ju, Y. W.; Hu, R.; Xie, Y.; Yao, J. P.; Li, X. X.; Lv, Y. L.; Han, X. T.; Cao, Q. L.; Li, L. Reconfigurable Magnetic Soft Robots with Multimodal Locomotion. *Nano Energy* **2021**, *87*, 106169.
(33) Ze, Q.; Kuang, X.; Wu, S.; Wong, J.; Montgomery, S. M.; Zhang, R.; Kovitz, J. M.; Yang, F.; Qi, H. J.; Zhao, R. Magnetic Shape Memory Polymers with Integrated Multifunctional Shape Manipulation. *Adv. Mater.* **2020**, *32* (4), 1906657.
(34) Alapan, Y.; Karacakol, A. C.; Guzelhan, S. N.; Isik, I.; Sitti, M. Reprogrammable Shape Morphing of Magnetic Soft Machines. *Sci. Adv.* **2020**, *6* (38), No. eabc6414.
(35) Kuang, X.; Wu, S.; Ze, Q.; Yue, L.; Jin, Y.; Montgomery, S. M.; Yang, F.; Qi, H. J.; Zhao, R. Magnetic Dynamic Polymers for Modular Assembling and Reconfigurable Morphing Architectures. *Adv. Mater.* **2021**, *33* (30), 2102113.
(36) Zhang, J.; Ren, Z.; Hu, W.; Soon, R. H.; Yasa, I. C.; Liu, Z.; Sitti, M. Voxelated Three-Dimensional Miniature Magnetic Soft Machines via Multimaterial Heterogeneous Assembly. *Sci. Robot.* **2021**, *6* (53), No. eabf0112.
(37) Yang, X.; Shang, W. F.; Lu, H. J.; Liu, Y. T.; Yang, L.; Tan, R.; Wu, X. Y.; Shen, Y. J. An Agglutinate Magnetic Spray Transforms Inanimate Objects into Millirobots for Biomedical Applications. *Sci. Robot.* **2020**, *5* (48), No. eabc8191.
(38) Dong, Y.; Wang, L.; Xia, N.; Yang, Z.; Zhang, C.; Pan, C.; Jin, D.; Zhang, J.; Majidi, C.; Zhang, L. Untethered Small-Scale Magnetic Soft Robot with Programmable Magnetization and Integrated Multifunctional Modules. *Sci. Adv.* **2022**, *8* (25), No. eabn8932.
(39) Kim, S. K.; Wie, J. J.; Mahmood, Q.; Park, H. S. Anomalous Nanoinclusion Effects of 2D MoS_2 and WS_2 Nanosheets on the Mechanical Stiffness of Polymer Nanocomposites. *Nanoscale* **2014**, *6*, 7430−7435.
(40) Sun, B. N.; Jia, R.; Yang, H.; Chen, X.; Tan, K.; Deng, Q.; Tang, J. D. Magnetic Arthropod Millirobots Fabricated by 3D-Printed Hydrogels. *Adv. Intell.* **2022**, *4* (1), 2100139.
(41) Tasoglu, S.; Diller, E.; Guven, S.; Sitti, M.; Demirci, U. Untethered Micro-Robotic Coding of Three-Dimensional Material Composition. *Nat. Commun.* **2014**, *5*, 3124.

https://doi.org/10.1021/acsami.2c14180
ACS Appl. Mater. Interfaces 2022, 14, 52370−52378